Journal of Zhejiang University-SCIENCE B (Biomedicine & Biotechnology)
ISSN 1673-1581 (Print); ISSN 1862-1783 (Online)
www.jzus.zju.edu.cn; www.springerlink.com
E-mail: jzus@zju.edu.cn

Proteomic analysis of human umbilical vein endothelial cells exposed to $PM_{2.5}$*

Ji ZHU[1], Lin-wen-si ZHU[3], Jin-huan YANG[2], Ying-ling XU[2],
Cui WANG[2], Zhuo-yu LI[2], Wei MAO[4], De-zhao LU[†‡2]

[1]*Clinical Laboratory, the Third Affiliated Hospital of Zhejiang Chinese Medical University, Hangzhou 310053, China*
[2]*College of Life Science, Zhejiang Chinese Medical University, Hangzhou 310053, China*
[3]*School of Medicine, Shanghai Jiao Tong University, Shanghai 200240, China*
[4]*Cardiovascular Department, the First Affiliated Hospital of Zhejiang Chinese Medicine University, Hangzhou 310006, China*
[†]E-mail: ludezhao@126.com

Received Feb. 24, 2017; Revision accepted June 16, 2017; Crosschecked May 14, 2018

Abstract: Exposure to fine ambient particulate matter ($PM_{2.5}$) is known to be associated with cardiovascular disease. To uncover the molecular mechanisms involved in cardiovascular toxicity of $PM_{2.5}$, we investigated alterations in the protein profile of human umbilical vein endothelial cells (HUVECs) treated with $PM_{2.5}$ using two-dimensional electrophoresis in conjunction with mass spectrometry (MS). A total of 31 protein spots were selected as differentially expressed proteins and identified by matrix-assisted laser desorption/ionization-time of flight (MALDI-TOF) MS. The results demonstrated that DNA damage and cell apoptosis are important factors contributing to $PM_{2.5}$-mediated toxicity in HUVECs. It is further proposed that $PM_{2.5}$ can inhibit superoxide dismutase (SOD) activity and increase reactive oxygen species (ROS) and malonaldehyde (MDA) production in a concentration-dependent manner. Induction of apoptosis and DNA damage through oxidative stress pathways may be one of the key toxicological events occurring in HUVECs under $PM_{2.5}$ stress. These results indicated that the toxic mechanisms of $PM_{2.5}$ on cardiovascular disease are related to endothelial dysfunction.

Key words: Fine ambient particulate matter ($PM_{2.5}$); Human umbilical vein endothelial cell (HUVEC); Proteomics; Toxic mechanism
https://doi.org/10.1631/jzus.B1700103 **CLC number:** X511

1 Introduction

Industrialization, urbanization, and increases in the population are resulting in pollution of the environment (Nicolas et al., 2008). Deterioration of urban air quality has become an increasing and widespread concern throughout the world (Singh and Sharma, 2012). $PM_{2.5}$, the fine air particle with an aerodynamic diameter less than 2.5 μm, is the pollutant with the most undesired health effects (Brook et al., 2010; Zhang et al., 2018). The surface of $PM_{2.5}$ can also absorb large quantities of harmful substances such as sulfates, heavy metals, and organic and inorganic compounds. It can penetrate deeply into the alveolar ducts through the respiratory tract, even through the interstitial lung, and transfer into the circulatory system. Thus, it can seriously harm human health (Terzano et al., 2010).

Extensive evidence from epidemiological investigations has shown that acute and chronic exposure to fine ambient particulate matter ($PM_{2.5}$) is

‡ Corresponding author
* Project supported by the Medical and Health Science and Technology Fund of Zhejiang Province (No. 2016KYB224) and the Scientific Research Fund of Zhejiang Chinese Medicine University (No. 2015ZG17), China
ORCID: De-zhao LU, https://orcid.org/0000-0001-5227-6445

associated with cardiovascular disease (Burnett et al., 1999; Lee et al., 2014). It can increase the incidence and mortality of cardiovascular disease in hypertension, coronary heart disease, and diabetes mellitus patients (Pope et al., 2004; Vallejo et al., 2006; Cheng et al., 2017). In May 2010, the American Heart Association (AHA) officially noted that there was a clear causal relationship between the exposure of fine particles and the incidence and mortality of cardiovascular disease, and the impact of $PM_{2.5}$ on cardiovascular disease has become a serious public health problem in the world (Brook et al., 2010).

Vascular endothelial cell (VEC), a barrier between blood and blood vessel wall, is widely distributed in the body. It can produce and secrete a variety of bioactive substances and plays an important role in the regulation of vascular tone and vascular smooth muscle growth, the modulation of the adhesion of VECs and inflammatory cells, and the inhibition of platelet aggregation (Lu and Daugherty, 2013). Therefore, vascular endothelial dysfunction is considered to be the initial step in atherosclerosis.

Previous studies have demonstrated that elevated concentrations of ambient $PM_{2.5}$ are significantly related to increased mean pulmonary arterial pressure and markers of endothelial dysfunction in children (Calderón-Garcidueñas et al., 2008). Healthy adults exercising for 30 min near main traffic roads can develop endothelial-dependent vascular diastolic dysfunction, which indicates that $PM_{2.5}$ can enter into the circulatory system through alveoli and has a direct effect on the VECs (Rundell et al., 2007). The direct effects of the soluble organic fraction of $PM_{2.5}$ on the fibrinolytic function of endothelial cells were detected using rat heart microvessel endothelial cells exposed to organic extracts of diesel exhaust particles (OE-DEP) and urban fine particles (OE-UFP). The results showed that OE-DEP and OE-UFP exposure reduced the production of plasminogen activator inhibitor-1 (PAI-1). This mechanism was related to oxidative stress and was independent of oxygenase-1 (HO-1) activity (Hirano et al., 2003). After being exposed to different concentrations of $PM_{2.5}$, the ECV304 cell survival rate and intracellular superoxide dismutase (SOD) and glutathione (GSH) were decreased in a dose-dependent manner (Rundell et al., 2007).

Therefore, vascular endothelial dysfunction is one of the important mechanisms in $PM_{2.5}$-induced cardiovascular toxicity (Li et al., 2014; Wang et al., 2017). The real biological mechanism underlying the correlation between $PM_{2.5}$ exposure and endothelial dysfunction is not yet clear. As we all know, proteins are crucial for our health, and they play an important role in living systems and are essential to almost all life activities. Alterations in the protein activity or content, which are caused by environmental, physiological, or pathological conditions, can cause any adaptive responses (Alaoui-Jamali and Xu, 2006). Proteomics is regarded as a powerful tool to explore the cellular responses to $PM_{2.5}$, which can provide effective data for toxicological studies. Therefore, we mainly analyzed the proteomic alterations in human umbilical vein endothelial cells (HUVECs) after they were exposed to $PM_{2.5}$ in order to explore the mechanism of $PM_{2.5}$-induced endothelial dysfunction.

2 Materials and methods

2.1 Materials

Airborne $PM_{2.5}$ was kindly donated by Professor LI (Institute of Environmental Science, Shanxi University, Taiyuan, China). $PM_{2.5}$ was collected on the rooftop of a 5-storey building (approximately 25 m above ground) at Shanxi University. This site is located approximately 300 m away from a major roadway (Wucheng Road). There are no obvious industrial pollution sources around. Thus, the observations could be typical of the general urban pollution in Taiyuan (Li et al., 2014). For exposure in vitro, airborne $PM_{2.5}$ was dissolved in sterilized water at a final concentration of 10 mg/ml and sonicated 30 min before use.

2.2 Cell culture

HUVECs were purchased from the Type Culture Collection of the Chinese Academy of Sciences (Shanghai, China). Cells were grown in Dulbecco's modified Eagle's medium (DMEM) supplemented with 10% (0.1 g/ml) heat-inactivated foetal bovine serum (FBS) and 1% (0.01 g/ml) penicillin-streptomycin and maintained at 37 °C in a humidified atmosphere of 5% CO_2. The study was performed when cells reached 70%–80% confluence.

2.3 Cell viability

Cells (1×10^4 cells/well) were seeded into 96-well plates and adhered to the well after 16 h. Then, the cells were treated with 10–150 μg/ml $PM_{2.5}$ for 24 h; cells in the control group were not treated with $PM_{2.5}$, and the blank group contained neither cells nor $PM_{2.5}$. Cell viability was measured using a 3-(4,5-dimethylthiazol-2-yl)-2,5-diphenyl tetrazolium bromide (MTT) assay kit (Keygen, China) according to the manufacturer's instructions. MTT (20 μl, 5 mg/ml) was added to every well and incubated for 4 h at 37 °C in a humidified atmosphere of air plus 5% CO_2. Then, 150 μl of dimethyl sulfoxide (DMSO) was added to solubilize the formazan salt formed, and the amount was determined spectrophotometrically at 570 nm using a SpectraMax190 microplate reader (Molecular Devices Inc., USA). Relative cell mass was determined from the amount of MTT converted to formazan salt.

2.4 Preparation of protein samples for two-dimensional (2-D) electrophoresis

HUVECs (1×10^6) were seeded into 75-cm^2 culture flasks with supplemented culture medium. The cells at exponential phase were then treated with 0, 50, and 100 μg/ml $PM_{2.5}$ for 24 h. Cells were harvested by centrifugation at 1500*g* for 10 min and lysed in 1 ml of lysis buffer (30 mmol/L Tris, 8 mol/L urea, 4% (0.04 g/ml) 3-[(3-cholamidopropyl)dimethylammonio]-1-propanesulfonic acid (CHAPS), 1% (0.01 g/ml) protease inhibitor, at pH 8.5). The sample solutions were gently mixed and kept on ice for 15 min with sonication for 10 s every 20 s and then centrifuged at 12000 r/min for 30 min at 4 °C. The supernatant was collected, and its protein concentration was determined using the bicinchoninic acid (BCA) protein assay (Solarbio Science & Technology, Beijing, China). The procedure was repeated twice, and a pool of extract was analyzed. The samples were stored at −80 °C until use.

2.5 2-D electrophoresis and image analysis

Samples (300 μg per gel) were loaded onto 24-cm Immobiline Dry strips with a pH 4–7 gradient (GE Healthcare, USA), and isoelectric focusing was carried out using an Ettan IPGphor 3 IEF system (GE Healthcare, USA). After isoelectric focusing, the strips were equilibrated for 15 min in a buffer containing 6 mol/L urea, 30% (0.3 g/ml) glycerol, and 1% (0.01 g/ml) dithiothreitol (DTT) and for 15 min in the same buffer but with DTT replaced by 4% (0.04 g/ml) iodoacetamide. The second-dimensional sodium dodecyl sulfate polyacrylamide gel electrophoresis (SDS-PAGE) was carried out on all 6 gels simultaneously using Ettan DALTsix (GE Healthcare, USA) at 5 W/strip for 45 min and then at 15 W/strip until the bromophenol blue reached the bottom of the polyacrylamide gels. The spots were stained with the sensitive silver staining and scanned with Image Scanner (GE Healthcare, USA) at 300 pixels per square inch, and the maps were analyzed using Image Master 2D Platinum 6.0 software (GE Healthcare, USA). Triplicate gels for each group were used to reduce experimental errors. Protein with average increase or decrease more than 1.5-fold compared with the control group was designated as differentially expressed protein and identified with a matrix-assisted laser desorption/ionization time-of-flight (MALDI-TOF) mass spectrometer (Applied Biosystem, USA).

2.6 In-gel digestion and MALDI-TOF mass spectrometry (MS) identification

Differentially expressed proteins were excised from the gels and de-stained by washing with a 1:1 solution of 100 mmol/L sodium thiosulfate and 30 mmol/L potassium ferricyanide for 20 min. The spots were dehydrated by addition of acetonitrile after being washed twice in Milli-Q water followed by drying in a Speed Vacuum (Eppendorf, USA) for 30 min. Subsequently, the gel spots were rehydrated in 5 μl of trypsin solution (20 ng/μl) and incubated at 37 °C for 16 h. Next, peptides were extracted in two washing steps with 50% (v/v) acetonitrile and 5% (v/v) trifluoroacetic acid for 1 h and dried in a Speed Vacuum. A 1-μl aliquot of peptide mixture was mixed with an equal volume of 10 mg/ml cyano-4-hydroxycinnamic acid (Sigma, USA) and analyzed using MALDI-TOF MS (4800 Proteomics Analyzer, Applied Biosystem, USA). Positive MS reflector mode was used to acquire data from 900 to 4000 Da, and the spectra were used to automatically search the NCBI or protein database using Mascot software (Applied Biosystem, USA) (Vallejo et al., 2006).

2.7 Western blotting

Proteins (20 μg/sample) were resolved on 10% (0.1 g/ml) polyacrylamide gels by SDS-PAGE and then transferred to polyvinylidene fluoride (PVDF) membranes. The membranes were blocked with 5% non-fat dry milk in Tris-buffered saline with Tween 20 (TBST) for 1 h at room temperature and incubated overnight at 4 °C with primary antibodies against β-actin (CWbio, Beijing, China), Mer11A, Rad50, and Rad51 (Abcam, Cambridge, UK) at 1:1000 dilution and primary antibodies against heterogeneous nuclear ribonucleoprotein H1 (HNRNPH1) and enolase (Santa, Cruz Biotechnology) at 1:400 dilution. After washing with TBST, the membranes were incubated with secondary antibody, and immunoblotting was visualized using a ChemiScope series (Clinx Science Instruments Co., Ltd., Shanghai, China). Normalization involved blotting the same samples with mouse anti-actin.

2.8 Cell apoptosis assay

To further explore whether $PM_{2.5}$ causes the apoptosis of HUVECs, an Annexi V-fluorescein isothiocyanate (FITC) Apoptosis Detection kit (Beyotime, Beijing, China) was used to distinguish normal, apoptotic, and necrotic cells. HUVECs (2×10^5 cells/well) were plated on 6-well plates and treated with 0, 50, and 100 μg/ml $PM_{2.5}$ for 24 h; and then, the cells were collected and detected by flow cytometry according to the manufacturer's instructions.

2.9 Detection of 8-hydroxy-2'-deoxy-guanosine

8-Hydroxy-2'-deoxy-guanosine (8-OHdG), a biomarker of DNA base-modified product, was detected using an enzyme-linked immunosorbent assay (ELISA) kit (AmyJet Scientific, Wuhan, China). After 24 h of treatment with $PM_{2.5}$, HUVECs were harvested and washed twice with PBS. Cells were suspended in PBS (pH 7.4) and homogenized by sonication and centrifuged at 3000 r/min for 20 min, and then the supernatant was collected to measure the 8-OHdG content according to the manufacturer's protocol.

2.10 Detection of DNA double strand breaks (DSBs) by immunofluorescence assay

HUVECs were cultured on sterile glass coverslips overnight at 37 °C, and exposed with 0, 50, and 100 μg/ml $PM_{2.5}$, respectively, for 24 h. Then the cells were fixed with 4% paraformaldehyde for 15 min and incubated with 0.2% Triton X-100 at 4 °C for 15 min. After washes with PBS, the samples were blocked with goat serum to suppress nonspecific binding of IgG for 2 h, and incubated with γH2AX antibody for 2 h. The samples were washed three times and incubated for 1 h with FITC-conjugated secondary antibody, and then washed with PBS and incubated with nuclei dye (4',6-diamidino-2-phenylindole (DAPI)) for 15 min in a dark chamber. After washing with PBS and mounting on a coverslip with 90% glycerol, images were taken from the specimens using a fluorescence microscope (Leica DMi8, Germany).

2.11 Measurement of reactive oxygen species

Intracellular reactive oxygen species (ROS) production in HUVECs was measured by 2',7'-dichloro-dihydro-fluorescein diacetate (DCHF-DA, 10 μmol/L; Beyotime, China). The cells were treated with DCFH-DA for 30 min at 37 °C and immediately washed three times with PBS. The fluorescence intensity was read by a fluorescence microplate reader at 485 nm excitation and 525 nm emission wavelengths, and images were captured by a multifunctional fluorescence microscope (Leica DMi8, Germany).

2.12 Measurement of SOD activity and MDA production

Both SOD activity and malonaldehyde (MDA) production were measured with commercial kits (Beyotime Biotechnology, Shanghai, China) according to the manufacturer's protocols. Cells were treated with an ultrasonic homogenizer. SOD activity was determined from the absorbance at 560 nm, which was detected using a microplate reader (Molecular Devices, USA), and the results were averaged and expressed as U/mg of sample protein. The absorbance of MDA production was detected at 532 nm. The MDA concentration was calculated using absorbance complex and expressed as nmol/mg of protein. Both assays were performed in triplicate.

2.13 Statistical analysis

Experimental data were expressed as mean± standard deviation (SD). GraphPad Prism 5 was used to analyze the data, Student's *t*-test was used to assess

the significant differences between the treatment groups and the control group, and the *P*-value was set at 0.05.

3 Results

3.1 Effects of $PM_{2.5}$ on the proliferation of HUVECs

HUVECs were treated with various concentrations of $PM_{2.5}$ for 24 h, and the cell proliferation was evaluated by the MTT assay. $PM_{2.5}$ was found to inhibit HUVECs proliferation in a concentration-dependent manner when its concentration was greater than 50 μg/ml (Fig. 1).

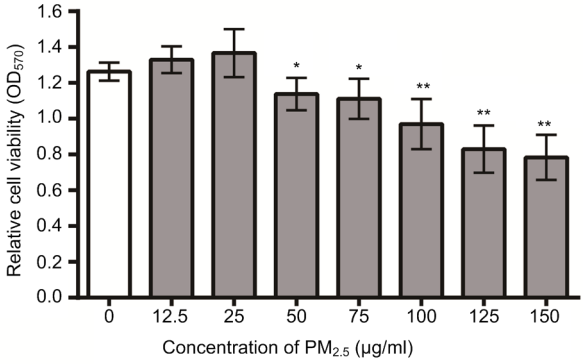

Fig. 1 Effect of $PM_{2.5}$ on the cell viability by MTT method

HUVECs were treated with the indicated concentrations of $PM_{2.5}$ for 24 h. Data are expressed as the mean±SD of triplicate experiments. * $P<0.05$, ** $P<0.01$, compared with the control

3.2 2-D gel electrophoresis analysis of differential protein expression

To elucidate the $PM_{2.5}$-induced alterations of protein expression in HUVECs, proteins extracted from the cells treated with $PM_{2.5}$ of different concentrations were separated by 2-D electrophoresis. Image analysis software (Image Master 2D, Version 6.0, GE Healthcare, USA) typically detected about 1000 proteins on each gel. The results showed that a total of 31 proteins exhibited statistically significant changes (increase or decrease, $P<0.05$), and the variations in abundance were more than 1.5-fold in contrast to the control cells. Among them, thirteen proteins were up-regulated in $PM_{2.5}$-treated HUVECs, while eighteen proteins were down-regulated. Fig. 2 shows the positions of differentially expressed proteins in master gel.

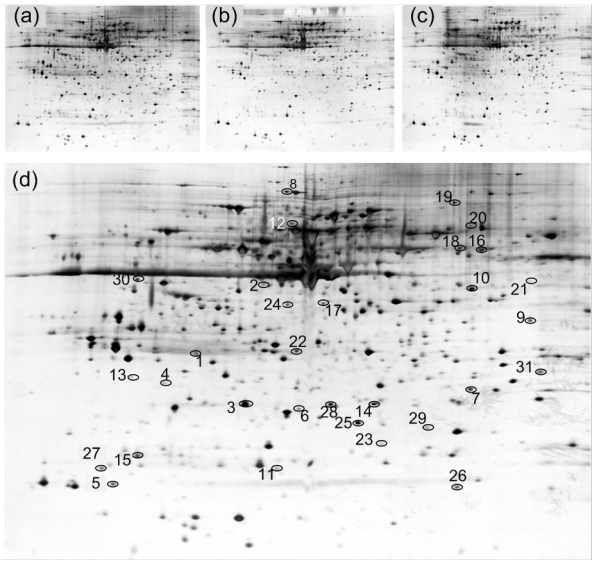

Fig. 2 Representative proteomic maps showing the protein expression profiles obtained from HUVECs exposed to $PM_{2.5}$

Proteomic maps of HUVECs treated with 0 (a), 50 (b), and 100 μg/ml (c) $PM_{2.5}$ for 24 h. (d) Distribution of differentially expressed proteins in master gel which has the maximum protein points among all gels

3.3 Identification of differentially expressed proteins

All of the differentially expressed proteins were further identified using MALDI-TOF MS. The MALDI-TOF MS peptide maps of in-gel tryptic digest resulting from HNRNPH1 are shown in Fig. 3. Table 1 lists the protein names, accession numbers, protein names, scores, and fold changes of these molecules. Table 2 shows the biological procession clustering of differentially expressed proteins in HUVECs treated with $PM_{2.5}$. As a result, HNRNPH1, ENO1, DYNC1H1, ST20, ZSCAN5A, CRK, PSMA3, and ZNF812 were related with DNA damage and RNA processing, which suggests the importance of DNA damage and RNA processing in $PM_{2.5}$-induced cytotoxicity. In addition, the expression changes of some proteins, including HNRNPH1, ENO1, FGG, DYNC1H1, ARHGDIA, PSMA3, and ST20, also indicate that apoptosis is one of the important toxic effects of $PM_{2.5}$.

3.4 Verification of differentially expressed proteins

HNRNPH1 and ENO1 expression was measured by Western blotting, using the β-actin protein band as a homogeneous control, which was useful for analyzing the experimental data. A comparison of the Western blotting results was consistent with our different proteomic analysis (Fig. 4).

Table 1 Information of differentially expressed proteins

Spot No.	Protein name	Accession No.	pI/MW	Mascot score/CI%	Fold changes	
					50 μg/ml vs. control	100 μg/ml vs. control
1	Calpain small subunit 1 (CAPNS1)	sp|P04632|CPNS1_HUMAN	5.05/28297.7	180/100.00	2.88	3.21
2	β-Actin-like protein (ACTBL2)	sp|Q562R1|ACTBL_HUMAN	5.39/41976.0	86/100.00	2.49	2.98
3	Rho GDP-dissociation inhibitor 1 (ARHGDIA)	sp|P52565|GDIR1_HUMAN	5.02/23192.7	86/100.00	−2.38	−2.76
4	Tumor protein D52 (TPD52)	sp|P55327|TPD52_HUMAN	4.79/24312.2	50/81.50	2.13	2.65
5	Cytoplasmic dynein 1 heavy chain 1 (DYNC1H1)	sp|Q14204|DYHC1_HUMAN	6.01/532071.8	60/98.00	−2.04	−2.12
6	Fibrinogen gamma chain (FGG)	sp|P02679|FIBG_HUMAN	5.37/51478.9	98/100.00	−1.98	−2.35
7	α/β Hydrolase domain-containing protein 14B (ABHD)	sp|Q96IU4|ABHEB_HUMAN	5.94/22331.6	66/99.53	−1.94	−2.29
8	Heat shock 70 kDa (HSP70) protein 4 (HSPA4)	sp|P34932|HSP74_HUMAN	5.11/94271.2	65/99.39	−1.84	−1.97
9	Ras-related protein Rab-14 (RAB14)	sp|P61106|RAB14_HUMAN	5.85/23881.9	47/56.66	1.73	1.92
10	Uracil phosphoribosyltransferase homolog (UPRT)	sp|Q96BW1|UPP_HUMAN	5.71/33765.0	39/78.00	1.71	2.10
11	F-box only protein 4 (FBX 4)	sp|Q9UKT5|FBX4_HUMAN	5.77/44108.0	33/45.00	−1.68	−1.59
12	tRNA methyltransferase 112 homolog (TRMT112)	sp|Q9UI30|TR112_HUMAN	5.21/14190.3	67/69.00	1.65	1.87
13	Zinc finger and SCAN domain-containing protein 5A (ZSCAN5A)	sp|Q9BUG6|ZSA5A_HUMAN	8.70/55829.8	42/49.00	−1.65	−1.77
14	MAGUK p55 subfamily member 2 (MPP2)	sp|Q14168|MPP2_HUMAN	6.32/64540.2	51/84.26	−1.65	−1.83
15	Myosin regulatory light chain 12A (MYL12A)	sp|P19105|ML12A_HUMAN	4.67/19781.5	176/100.00	−1.64	−1.91
16	Heterogeneous nuclear ribonucleoprotein H (HNRNPH1)	sp|P31943|HNRH1_HUMAN	5.89/49198.4	178/100.00	1.63	1.65
17	Adapter molecule crk (CRK)	sp|P46108|CRK_HUMAN	5.38/33810.0	152/100.00	1.53	2.19
18	Filamin-A-interacting protein 1 (FILIP1)	sp|Q7Z7B0|FLIP1_HUMAN	8.46/138023.9	51/83.14	1.52	1.76
19	Protein monoglycylase Tubulin-tyrosine ligase-like protein 8 (TTLL8)	sp|A6PVC2|TTLL8_HUMAN	8.55/94616.0	44/19.29	1.77	1.74
20	Exocyst complex component 6B (EXOC6B)	sp|Q9Y2D4|EXC6B_HUMAN	6.03/94141.1	48/63.95	1.58	1.64
21	α-Enolase (ENO1)	sp|P06733|ENOA_HUMAN	7.01/47139.3	61/98.00	1.58	1.52
22	Proteasome subunit α type-3 (PSMA3)	sp|P25788|PSA3_HUMAN	5.19/28415.1	81/99.98	−1.62	−1.53
23	Neural cell adhesion molecule 2 (NCAM2)	sp|O15394|NCAM2_HUMAN	5.44/92988.2	46/46.68	−1.63	−1.54
24	Proteasome subunit β type-2 (PSMB2)	sp|P49721|PSB2_HUMAN	6.51/22821.7	87/89.00	−1.58	−1.55

To be continued

Table 1

Spot No.	Protein name	Accession No.	pI/MW	Mascot score/CI%	Fold changes	
					50 ug/ml vs. control	100 ug/ml vs. control
25	Zinc finger CCCH domain-containing protein 7B (ZC3H7B)	sp|Q9UGR2|Z3H7B_HUMAN	6.82/111506.5	48/64.77	−1.68	−1.61
26	Transcription factor-like 5 protein (TCFL5)	sp|Q9UL49|TCFL5_HUMAN	6.44/52664.2	48/65.57	−1.69	−1.82
27	Suppressor of tumorigenicity 20 protein (ST20)	sp|Q9HBF5|ST20_HUMAN	8.52/9017.6	48/71.36	−1.74	−1.85
28	Putative zinc finger protein 812 (ZNF812)	sp|P0C7V5|ZN812_HUMAN	8.71/51484.2	65/99.39	−1.53	−2.15
29	Deoxyuridine 5'-triphosphate nucleotidohydrolase (DUT)	sp|P33316|DUT_HUMAN	9.46/26546.6	80/99.98	−2.12	−3.21
30	Reticulocalbin-1 (RCN1)	sp|Q15293|RCN1_HUMAN	4.86/38866.2	114/100.00	−2.39	−4.37
31	Putative malate dehydrogenase 1B (MDH1B)	sp|Q5I0G3|MDH1B_HUMAN	5.85/58613.4	56/78.00	−2.47	−4.39

pI: isoelectric point; MW: molecular weight; CI%: minimum ion score

Table 2 Determination of toxicity rank

Biological procession	Protein name
DNA damage and RNA processing	HNRNPH1, ENO1, PSMA3, DYNC1H1, ST20, ZSCAN5A, CRK, ZNF812
Cell apoptosis	HNRNPH1, ENO1, PSMA3, ST20, DYNC1H1, FGG, ARHGDIA
Cell proliferation	CAPNS1, TPD52, ENO1, PSMA3
Cell adhesion and platelet aggregation	ARHGDIA, FGG, MYL12A, CRK, NCAM2
Cell cycle	DYNC1H1, PSMA3

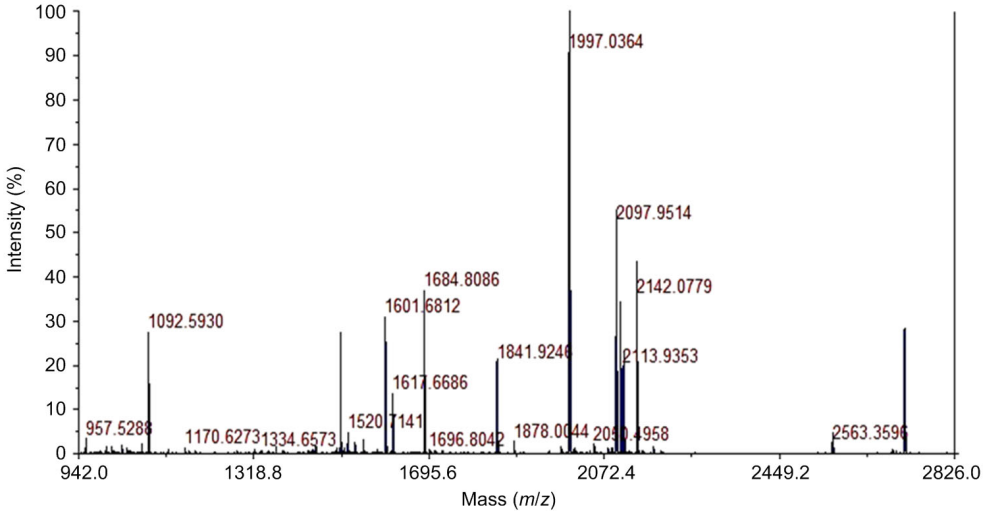

Fig. 3 MALDI-TOF MS peptide maps of HNRNPH1

Protein spot of interest was excised from the gels and de-stained, washed, dehydrated, and enzymolyzed. Peptides were extracted and freeze-dried. The peptide mixture was analyzed with MALDI-TOF MS

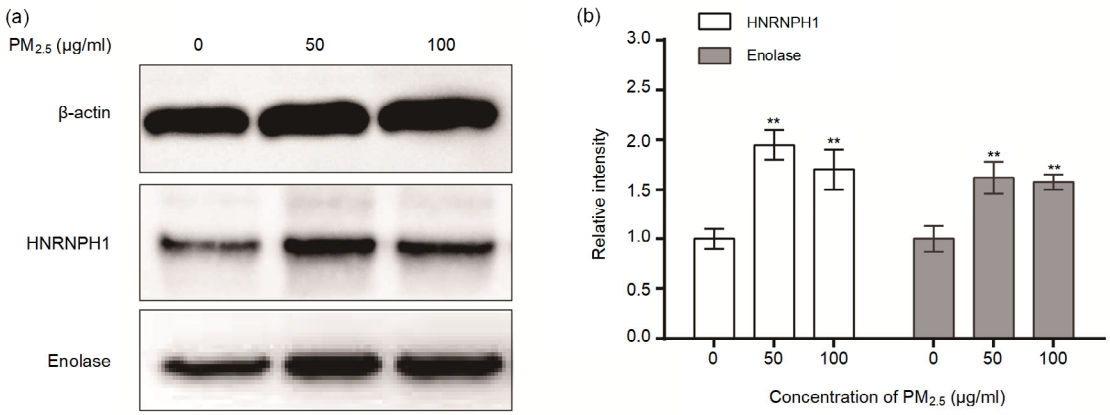

Fig. 4 Western blot analysis of representative protein of differentially expressed proteins

(a) Expression of HNRNPH1 and enolase (ENO1) in HUVECs treated with 0, 50, and 100 μg/ml $PM_{2.5}$ for 24 h. (b) Relative intensities of HNRNPH1 and ENO1 were quantified. Data are expressed as the mean±SD of triplicate experiments. ** $P<0.01$, compared with the control

3.5 $PM_{2.5}$-induced apoptosis in HUVECs

Flow cytometry was used to detect the proportion of apoptosis in total cells to verify whether $PM_{2.5}$ induced apoptosis in HUVECs. The results showed that the percentage of early apoptosis (Annexin V^+/PI^- (PI: propidium iodide)) increased to 17.3% and 25.5%, respectively, compared to 1.7% in the control cells when the HUVECs treated with 50 and 100 μg/ml $PM_{2.5}$ for 24 h (Fig. 5).

3.6 DNA damage in HUVECs exposed to $PM_{2.5}$

After 24 h of treatment with $PM_{2.5}$, the cells were collected and broken by sonication and then centrifuged at 3000 r/min for 20 min; the supernatant was used for ELISA. As shown in Fig. 6, the DNA damage involving production of 8-OHdG was up-regulated at 100 μg/ml. The results indicated that $PM_{2.5}$ induced oxidative stress-related DNA damage.

3.7 Formation of DNA DSBs in HUVECs exposed to $PM_{2.5}$

$PM_{2.5}$-induced DNA DSBs in HUVECs were assayed by the formation of γH2AX foci after 24 h treatment with different concentrations of $PM_{2.5}$. The accumulated bright green spots were marked as the formation of γH2AX foci. A significant increase in foci number was detected in HUVECs treated with 50 and 100 μg/ml $PM_{2.5}$, which indicated that $PM_{2.5}$ can cause the DNA DSBs in HUVECs (Fig. 7).

3.8 Expression of DNA damage repair proteins

The expression of DNA damage repair proteins Mer11A, Rad50, and Rad51 was measured by Western blotting using β-actin protein band as a homogeneous control, which was useful for analyzing the experimental data. A comparison of the Western blotting results was consistent with our different proteomic analysis (Fig. 8).

3.9 $PM_{2.5}$-regulated oxidative stress in vitro

We evaluated the effects of $PM_{2.5}$ on oxidative stress of endothelial cells. The results showed that ROS generation was significantly increased after cell exposure to $PM_{2.5}$ (Fig. 9a). Consistently, $PM_{2.5}$ led to a more significant down-regulation of SOD activity and up-regulation of MDA expression (Figs. 9b and 9c). These results suggested that $PM_{2.5}$-induced apoptosis and DNA damage may be related to oxidative stress.

4 Discussion

Recent studies suggested that the increases of ambient particular matter levels were associated with an increase in mortality rate from cardiovascular disease. VECs, the first barrier between the blood and the vessel wall, play important roles in cardiovascular disease. VECs can produce and secrete a variety of bioactive substances to regulate vascular tone, smooth muscle cell proliferation, adhesion of VECs and inflammatory cells, and inhibit platelet aggregation (Lu and Daugherty, 2013).

Our study showed that $PM_{2.5}$ can inhibit HUVEC proliferation in a concentration-dependent manner. To elucidate the toxicology mechanism of $PM_{2.5}$ in

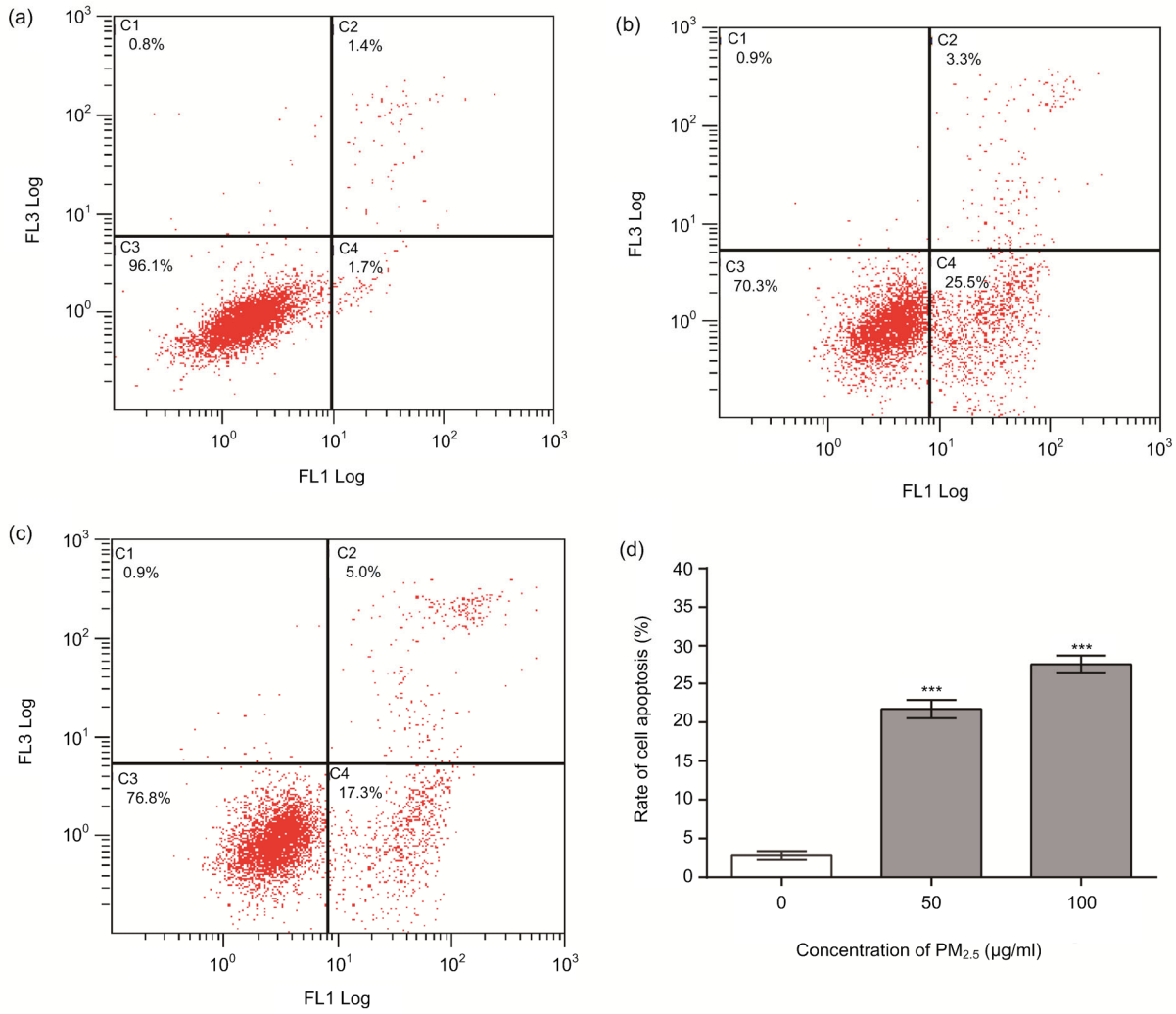

Fig. 5 Flow cytometry analysis of HUVECs by double labelling with Annexin-V fluorescein isothiocyanate (FITC) and propidium iodide (PI)

(a) Control group (0 μg/ml $PM_{2.5}$-treated group); (b) 50 μg/ml $PM_{2.5}$-treated group; (c) 100 μg/ml $PM_{2.5}$-treated group; (d) Mean percentages of the early stage apoptotic cells. Data are expressed as the mean±SD of triplicate experiments. *** $P<0.001$, compared with the control

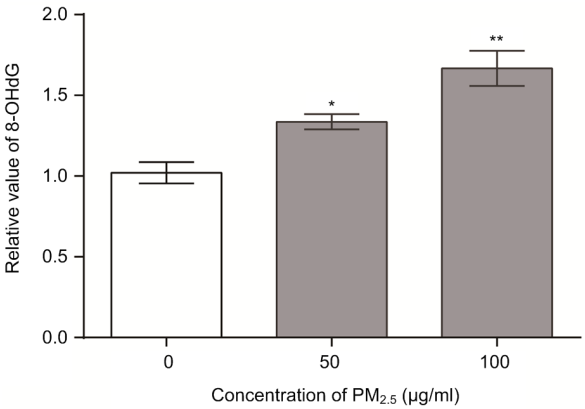

Fig. 6 Effects of $PM_{2.5}$ on DNA damage production 8-OHdG of HUVECs after 24 h treatment

Data are expressed as the mean±SD of triplicate experiments. * $P<0.05$, ** $P<0.01$, compared with the control

HUVECs, the comparative proteomic analysis was performed in our experiments to reveal the $PM_{2.5}$-induced proteins in HUVECs in order to accumulate novel toxicological data on environmental exposure to particulate matter. Thirty-one differentially expressed proteins related to exposure to $PM_{2.5}$ were selected and identified, of which eight proteins, namely, HNRNPH1, ENO1, DYNC1H1, ST20, ZSCAN5A, CRK, PSMA3, and ZNF812, were involved in DNA damage and RNA processing. As DNA damage is usually induced by oxidative stress and other stresses, which may be more representative of $PM_{2.5}$ toxicity, this was raised as a concern in our studies.

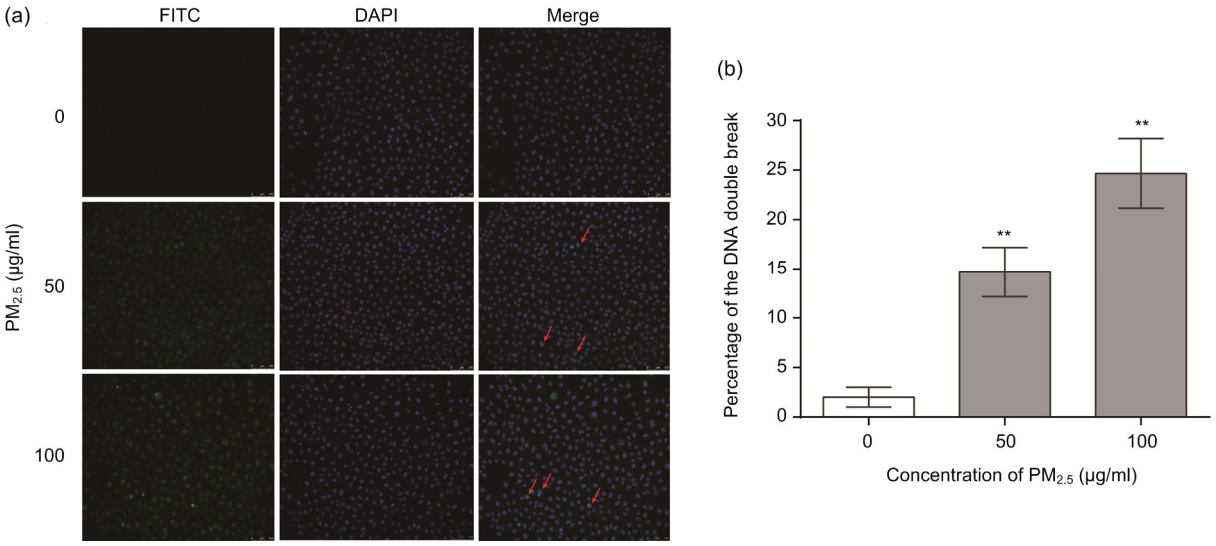

Fig. 7 $PM_{2.5}$-induced DNA DSBs in HUVECs treated with $PM_{2.5}$ at 0, 50, and 100 μg/ml

(a) Cells were fixed and processed for immunofluorescence assay by incubation with γH2AX antibody and nuclei dye DAPI. The arrows represent the formation of γH2AX foci. (b) Percentage of the DNA double break in HUVECs was quantified accurately. Data are expressed as the mean±SD of triplicate experiments. ** P<0.01, compared with the control

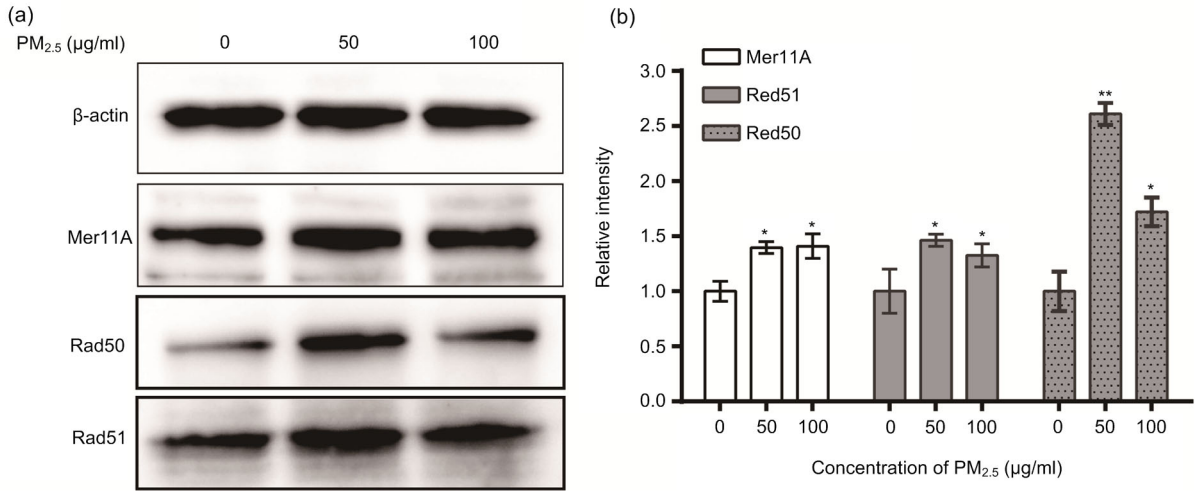

Fig. 8 Western blot analysis of representative DNA damage repair proteins

(a) Expression of DNA damage repair proteins in HUVECs treated with 0, 50, and 100 μg/ml $PM_{2.5}$ for 24 h. (b) Relative intensities of DNA damage repair proteins were quantified. Data are expressed as the mean±SD of triplicate experiments. * P<0.05, ** P<0.01, compared with the control

Oxidative stress is the damage of intracellular antioxidant defense system, and the accumulation of metabolite-related oxygen free radicals due to excessive oxygen free radical production results in a variety of pathological conditions (Brigelius-Flohe, 2009). Recent research shows that oxidative stress is one of the important causes of damage to cardiovascular system structure and function and is associated with a variety of cardiovascular diseases (Azad et al., 2009).

ROS, the most important molecules of oxidative stress, are produced in the body both through natural biological processes as well as in response to external stimuli such as air pollution. The mechanisms have evolved to maintain cellular redox equilibrium and to counter the potential adverse health effects of oxidative stress including damage to cellular macromolecules such as proteins and DNA, inflammation, and cytotoxicity (Li et al., 2003; Ghio et al., 2012). A number of antioxidant-related genes have been identified, and several studies have examined the degree to which polymorphisms in these genes may modify responses to $PM_{2.5}$ (Weichenthal et al., 2013).

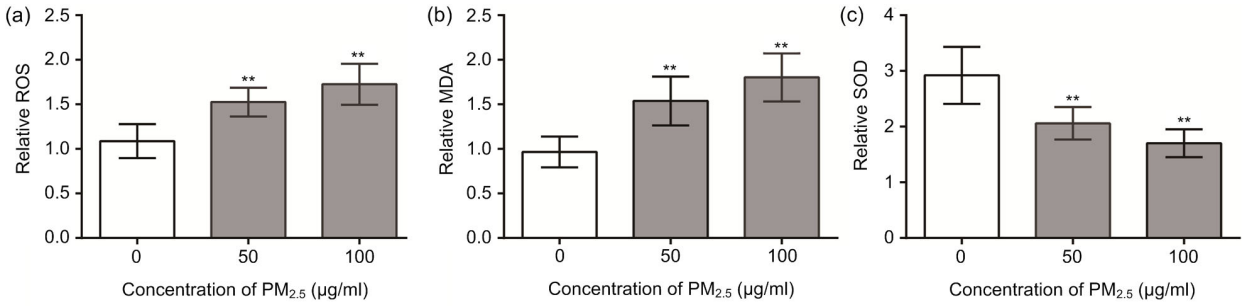

Fig. 9 $PM_{2.5}$-induced oxidative stress

(a) Intracellular ROS production was measured by DCF fluorescence microscopy and fluorescence was quantified. (b, c) SOD activity and MDA production were detected as products of oxidative stress. Data are expressed as the mean±SD of triplicate experiments. ** $P<0.01$, compared with the control

Polycyclic aromatic hydrocarbons in organic compounds and transition metals, the main component of $PM_{2.5}$, can increase reactive oxygen radicals and DNA damage (Torres-Ramos et al., 2011). It has been shown that the organic substances in $PM_{2.5}$ can lead to DNA adduct synthesis and oxidative DNA damage in vitro studies, which may result in gene mutation and formation of a tumour if the DNA damage is not repaired timely (Lee and Yang, 2012). The results of our experiment also showed that the levels of MDA and ROS increased while the activity of SOD decreased in HUVECs exposed to 50 or 100 μg/ml $PM_{2.5}$ for 24 h. In addition, 8-OHdG, a biological marker of oxidative damage to DNA by endogenous or exogenous factors, increased in $PM_{2.5}$-treated HUVECs, which indicated that $PM_{2.5}$ could induce DNA damage of VECs by increasing the generation of ROS.

Normally, cells will initiate different damage repair mechanisms according to the degree of DNA damage. The repair system can repair minor DNA in time, but severe DNA damage often leads to cell apoptosis and even generates oncogenic mutations. DSBs are the most important type of DNA damage, in which a double-stranded DNA molecule breaks in the relative position or adjacent number base. There are two mechanisms involved in DNA double-strand repair; one is homologous recombination (HR), and the other is non-homologous end joining (NHEJ). These two types of repair mechanisms involve a complex process of multiple repair proteins to maintain the stability of the genome, of which HR is of more interest to researchers. DNA damage repair protein 52 (Rad52) is the most important protein in HR, which can connect to the end of the DNA chain and promote the annealing of complementary chain. Under the action of Rad52, the homologous recombination repair complex (Rad50-Mre11-Nbs1) is connected to the fracture of DSBs and initiates the chain exchange reaction of DNA mediated by Rad51 protein. Up-regulation of the expression of Rad51, Rad50, and MRE11A in HUVECs exposed to $PM_{2.5}$ further demonstrates the role of $PM_{2.5}$ in inducing DNA damage.

In the different proteins involved in DNA damage, several proteins such as HNRNPH1, ENO1, and PSMA3 are also related to apoptosis. The HNRNPs are RNA-binding proteins that form a complex with heterogeneous nuclear RNA. HNRNPH1 has been implicated in various processes, including chromatin remodelling, DNA damage and repair, transcription, mRNA splicing, and protein translation, by interactions with a range of biomolecules related to the regulation of gene expression. Heterogeneous nuclear ribonucleoprotein F/H proteins modulate the alternative splicing of the apoptotic mediator Bcl-x. The addition of HNRNP to a HeLa extract improved the production of the pro-apoptotic Bcl-xS variant and small interfering RNA-mediated RNA interference targeting HNRNP F and H decreased the Bcl-xS/Bcl-xL ratio of plasmid-derived and endogenously produced Bcl-x transcripts (Garneau et al., 2005).

ENO1 is a key enzyme involved in sugar metabolism. In recent years, research has shown that ENO1 participates in the regulation of fibrinolytic enzyme activation and fibrinolytic enzyme activity processes, promoting muscle generation and muscle regeneration, and regulating the development process of cell apoptosis and tumour. Ucker et al. (2012) found that a large number of secretions of glycolytic

enzymes (especially ENO1) are common in early cell apoptosis. In apoptotic cells, ENO1 has lost its inherent glycolytic activity, but the original receptors can be used as a fibrinolytic enzyme involved in regulation of cell apoptosis process (Singh and Sharma, 2012). The proteasome is a multi-catalytic proteinase complex, which is characterized by its ability of cleaving peptides; however, proteasome also has the function of inhibiting cell apoptosis. PSMA3 is a proteasomal protein of the T1A peptidase family, which is involved in some biological processes such as transcription, replication, and DNA repair. In addition, a study has also shown that PSMA3 can increase the expression of Bim and induce cell apoptosis to some extent (Brook et al., 2010). Based on the apoptotic analysis with cytometry (Fig. 4), apoptosis is confirmed as one of the key mechanisms for $PM_{2.5}$ toxicity.

Our results also showed increased expression of TPD52 and decreased expression of suppressor of ST20 in the HUVECs exposed to 50 or 100 μg/ml $PM_{2.5}$. Transcriptional regulation of some oncogenic genes and tumour suppressor genes is also an important cause for cytotoxicity of $PM_{2.5}$.

In summary, considering the function of the different proteins in HUVECs under $PM_{2.5}$ stress and the result of experiments of DNA damage and cell apoptosis, we proposed that the modulation of several proteins such as HNRNPH1, ENO1, and PSMA3 contributes to the DNA damage induced by $PM_{2.5}$ and promotes cell apoptosis, which could result in endothelium dysfunction, the initial factor in atherosclerosis. In addition, our experiment also proposed the regulation of TPD52 and ST20 as key carcinogenic mechanisms for $PM_{2.5}$.

Compliance with ethics guidelines

Ji ZHU, Lin-wen-si ZHU, Jin-huan YANG, Ying-ling XU, Cui WANG, Zhuo-yu LI, Wei MAO, and De-zhao LU declare that they have no conflict of interest.

This article does not contain any studies with human or animal subjects performed by any of the authors.

References

Alaoui-Jamali MA, Xu YJ, 2006. Proteomic technology for biomarker profiling in cancer: an update. *J Zhejiang Univ-Sci B*, 7(6):411-420. https://doi.org/10.1631/jzus.2006.B0411

Azad MB, Chen YQ, Gibson SB, 2009. Regulation of autophagy by reactive oxygen species (ROS): implications for cancer progression and treatment. *Antioxid Redox Sign*, 11(4):777-790. https://doi.org/10.1089/ars.2008.2270

Brigelius-Flohe R, 2009. Commentary: oxidative stress reconsidered. *Genes Nutr*, 4(3):161-163. https://doi.org/10.1007/s12263-009-0131-8

Brook RD, Rajagopalan S, Pope CA, et al., 2010. Particulate matter air pollution and cardiovascular disease: an update to the scientific statement from the American Heart Association. *Circulation*, 121(21):2331-2378. https://doi.org/10.1161/CIR.0b013e3181dbece1

Burnett RT, Smith-Doiron M, Stieb D, et al., 1999. Effects of particulate and gaseous air pollution on cardiorespiratory hospitalizations. *Arch Environ Health*, 54(2):130-139. https://doi.org/10.1080/00039899909602248

Calderón-Garcidueñas L, Villarreal-Calderon R, Valencia-Salazar G, et al., 2008. Systemic inflammation, endothelial dysfunction, and activation in clinically healthy children exposed to air pollutants. *Inhal Toxicol*, 20(5):499-506. https://doi.org/10.1080/08958370701864797

Cheng Q, Yang CY, Guo BY, et al., 2017. Analysis of mechanism of PM2.5 and house dust mite antigen Der p1 in attack stage of child asthma. *Eur Rev Med Pharmacol Sci*, 21(10):2458-2462.

Garneau D, Revil T, Fisette JF, et al., 2005. Heterogeneous nuclear ribonucleoprotein F/H proteins modulate the alternative splicing of the apoptotic mediator Bcl-x. *J Biol Chem*, 280(24):22641-22650. https://doi.org/10.1074/jbc.M501070200

Ghio AJ, Carraway MS, Madden MC, 2012. Composition of air pollution particles and oxidative stress in cells, tissues, and living systems. *J Toxicol Environ Health Part B*, 15(1):1-21. https://doi.org/10.1080/10937404.2012.632359

Hirano S, Furuyama A, Koike E, et al., 2003. Oxidative-stress potency of organic extracts of diesel exhaust and urban fine particles in rat heart microvessel endothelial cells. *Toxicology*, 187(2-3):161-170. https://doi.org/10.1016/S0300-483X(03)00053-2

Lee BJ, Kim B, Lee K, 2014. Air pollution exposure and cardiovascular disease. *Toxicol Res*, 30(2):71-75. https://doi.org/10.5487/TR.2014.30.2.071

Lee IT, Yang CM, 2012. Role of NADPH oxidase/ROS in pro-inflammatory mediators-induced airway and pulmonary diseases. *Biochem Pharmacol*, 84(5):581-590. https://doi.org/10.1016/j.bcp.2012.05.005

Li N, Hao MQ, Phalen RF, et al., 2003. Particulate air pollutants and asthma: a paradigm for the role of oxidative stress in PM-induced adverse health effects. *Clin Immunol*, 109(3):250-265. https://doi.org/10.1016/j.clim.2003.08.006

Li RJ, Kou XJ, Geng H, et al., 2014. Pollution characteristics of ambient $PM_{2.5}$-bound PAHs and NPAHs in a typical winter time period in Taiyuan. *Chin Chem Lett*, 25(5):663-666. https://doi.org/10.1016/j.cclet.2014.03.032

Lu H, Daugherty A, 2013. Atherosclerosis: cell biology and lipoproteins. *Curr Opin Lipidol*, 24(1):107-108. https://doi.org/10.1097/MOL.0b013e32835c7bb7

Nicolas J, Chiari M, Crespo J, et al., 2008. Quantification of Saharan and local dust impact in an arid Mediterranean area by the positive matrix factorization (PMF) technique. *Atmos Environ*, 42(39):8872-8882. https://doi.org/10.1016/j.atmosenv.2008.09.018

Pope CA, Burnctt RT, Thurston GD, et al., 2004. Cardiovascular mortality and long-term exposure to particulate air pollution: epidemiological evidence of general pathophysiological pathways of disease. *Circulation*, 109(1):71-77. https://doi.org/10.1161/01.CIR.0000108927.80044.7F

Rundell KW, Hoffman JR, Caviston R, et al., 2007. Inhalation of ultrafine and fine particulate matter disrupts systemic vascular function. *Inhal Toxicol*, 19(2):133-140. https://doi.org/10.1080/08958370601051727

Singh R, Sharma BS, 2012. Composition, seasonal variation, and sources of PM_{10} from world heritage site Taj Mahal, Agra. *Environ Monit Assess*, 184(10):5945-5956. https://doi.org/10.1007/s10661-011-2392-0

Terzano C, Di Stefano F, Conti V, et al., 2010. Air pollution ultrafine particles: toxicity beyond the lung. *Eur Rev Med Pharmacol Sci*, 14(10):809-821.

Torres-Ramos YD, Montoya-Estrada A, Guzman-Grenfell AM, et al., 2011. Urban PM2.5 induces ROS generation and RBC damage in COPD patients. *Front Biosci*, 3:808-817.

Ucker DS, Jain MR, Pattabiraman G, et al., 2012. Externalized glycolytic enzymes are novel, conserved, and early biomarkers of apoptosis. *J Biol Chem*, 287(13):10325-10343. https://doi.org/10.1074/jbc.M111.314971

Vallejo M, Ruiz S, Hermosillo AG, et al., 2006. Ambient fine particles modify heart rate variability in young healthy adults. *J Expo Sci Environ Epidemiol*, 16(2):125-130. https://doi.org/10.1038/sj.jea.7500447

Wang JS, Tseng CY, Chao MW, 2017. Diesel exhaust particles contribute to endothelia apoptosis via autophagy pathway. *Toxicol Sci*, 156(1):72-83. https://doi.org/10.1093/toxsci/kfw237

Weichenthal SA, Godri-Pollitt K, Villeneuve PJ, 2013. $PM_{2.5}$, oxidant defence and cardiorespiratory health: a review. *Environ Health*, 12:40. https://doi.org/10.1186/1476-069X-12-40

Zhang HH, Li Z, Liu Y, et al., 2018. Physical and chemical characteristics of $PM_{2.5}$ and its toxicity to human bronchial cells BEAS-2B in the winter and summer. *J Zhejiang Univ-Sci B (Biomed & Biotechnol)*, 19(4):317-326. https://doi.org/10.1631/jzus.B1700123

中文概要

题　目：大气细颗粒物 $PM_{2.5}$ 对人脐静脉内皮细胞蛋白质组的影响

目　的：应用双向电泳及质谱技术分析 $PM_{2.5}$ 对人脐静脉内皮细胞（HUVEC）蛋白质组的影响，探讨 $PM_{2.5}$ 引起心血管毒性的潜在机制。

创新点：多项流行病学调查表明，$PM_{2.5}$ 与人类心血管疾病有密切关系，而血管内皮细胞是血管的第一道防线。本项目应用蛋白质组技术研究 $PM_{2.5}$ 对血管内皮细胞损伤的作用，并从 DNA 损伤的角度探讨了 $PM_{2.5}$ 心血管毒性机制，具有较好的创新性。研究结果可为 $PM_{2.5}$ 的危害分析提供基础数据，同时为 $PM_{2.5}$ 的防治提供新的依据及思路。

方　法：培养 HUVEC 细胞，分为正常组（正常培养的 HUVEC 细胞）、$PM_{2.5}$ 处理组（50、100 μg/ml $PM_{2.5}$ 处理 HUVEC 细胞 24 h）。双向电泳技术建立各组细胞蛋白质组图谱，质谱技术鉴定差异表达的蛋白质，流式细胞术分析细胞凋亡情况，酶联免疫吸附法（ELISA）检测 DNA 损伤产物 8-OHdG 的水平，荧光标记技术分析 DNA 双链断裂的形成，并用免疫印迹法（Western blotting）检测 DNA 损伤相关蛋白的表达。

结　论：经 $PM_{2.5}$ 处理 HUVEC 后，31 个蛋白表达发生了显著性的变化（图 2，表 1），其中 8 个蛋白质参与了 DNA 的损伤与 RNA 的编缉，7 个蛋白质与细胞凋亡有关（表 2）。进一步实验表明：$PM_{2.5}$ 能够促细胞凋亡（图 5），提高 DNA 损伤产物 8-OHdG 的含量（图 6），促进 DNA 双链断裂位点的形成（图 7），调节损伤修复相关蛋白（Mer11A、Rad50 和 Rad51）的表达（图 8），抑制超氧化物歧化酶（SOD）的活性，增加 HUVEC 细胞内活性氧（ROS）和丙二醛（MDA）的水平（图 9）。综上所述，$PM_{2.5}$ 能够通过调节一系列蛋白的表达，加重 HUVEC 细胞氧化应激水平，增加 DNA 损伤，促进细胞凋亡，造成内皮细胞损伤，从而导致心脑血管事件的发生。

关键词：$PM_{2.5}$；人脐静脉内皮细胞；蛋白质组；毒性机制